Measurement of the Two-Photon Exchange Contribution in ep Elastic Scattering Using Recoil Polarization

S. Kowalski, R. Suleiman (Spokesperson, Contact Person), S. Taylor

Massachusetts Institute of Technology

L. Pentchev (Spokesperson), C.F. Perdrisat (Spokesperson), M. Vanderhaeghen

College of William & Mary

R. Gilman (Spokesperson), C. Glashausser, X. Jiang, G. Kumbartzki, K. McCormick, R. Ransome

Rutgers University

A. Adeluyi, A.T. Katramatou, G.G. Petratos

Kent State University, Kent, OH 44242

A. Afanasev, D. Higinbotham, M.K. Jones, D. Mack

Jefferson Lab

J. Arrington

Argonne National Laboratory

L. Bimbot

Institut de Physique Nucléaire, Orsay, France

E. Brash

U. of Regina, Regina, CA

J. Calarco

University of New Hampshire

C.C. Chang

University of Maryland

M. Epstein, D. Margaziotis

California State University at Los Angeles

S. Frullani

INFN-ISS, Italy

Yu.M. Goncharenko, Yu.M. Melnick, A.P. Meschanin, K.E. Shestermanov., L.F. Soloviev and A.N. Vasiliev

Institut for High Energy Physics, Protvino, Russia

V.P. Kubarovsky

Rensselaer Polytechnic Institute and Jefferson Lab

P. Markowitz

Florida International University and Jefferson Lab

N. Piskunov, S. Nedev, D. Kirillov, I. Sitnik

Laboratory for High Energy, JINR, Dubna, Russia

Vina Punjabi, M. Khandaker, C. Salgado

Norfolk State University

R. Segel

Nortwestern University

E. Tomasi-Gustafsson

DAPNIA, Saclay, France

P. Ulmer

Old Dominion University

(December 3, 2003)

Abstract

Recent Jefferson Lab results confirm that Rosenbluth separation and polarization transfer techniques disagree on the proton elastic electric form factor G_E^p at large Q^2. *"This discrepancy is a serious problem as it generates confusion and doubt about the whole methodology of lepton scattering experiments"* [1]. Two-photon exchange processes are considered to be the most likely explanation. Model calculations and fits to the data indicate that few percent contributions – somewhat larger than expected – might change the Rosenbluth separation results significantly, while leaving the polarization transfer form factor results almost unchanged. High Q^2 *ep* data are needed as a constraint, so that the validity of this two-photon exchange explanation can be more seriously evaluated. We propose to measure the ε dependence at constant Q^2 of the recoil proton polarization in *ep* elastic scattering, performing two independent experiments simultaneously by measuring the induced polarization and the polarization transfer components at the same time.

The induced polarization p_y is identically zero in one-photon exchange due to time reversal invariance. A nonzero measurement of such a *T-odd* polarization observable is a clean signal for the imaginary part of the two-photon exchange amplitude. We present estimates that show that this spin component, while small, is large enough that it can be clearly shown to be nonzero.

The polarization transfer components will be measured simultaneously. An ε dependence different from that predicted assuming one-photon exchange is a clean signal for the real part of the two-photon exchange amplitude, and has direct implications for the Rosenbluth separations. We present estimates of a measurable ε dependence to the polarization components, and to the

form factor ratio derived from them assuming one-photon exchange. Furthermore, we show how one can perform a model-independent analysis of the polarization-transfer and cross-section data to extract the form factors and two-photon contribution. Most importantly, we propose a procedure for testing the ε independence of the form factors, thus examining the applicability of the lepton-nucleon scattering as a method to investigate the structure of the nucleon.

We request 25 days of beam time, to measure four ε points at $Q^2 = 3.2$ GeV^2, and to perform a high statistics calibration of the polarimeter, to determine false asymmetries so that the few percent induced polarizations can be measured. The experiment requires no new equipment. It has identical needs to E01-109, G_E^p-III in Hall C. We have shortened the time request by several days, assuming the experiments can be jointly scheduled, so that certain overheads and systematics checks are not needed. Running together with E01-109 also saves the several weeks that would be needed for re- and de- installation of the electron calorimeter and HMS FPP.

I. MOTIVATION

A. Background

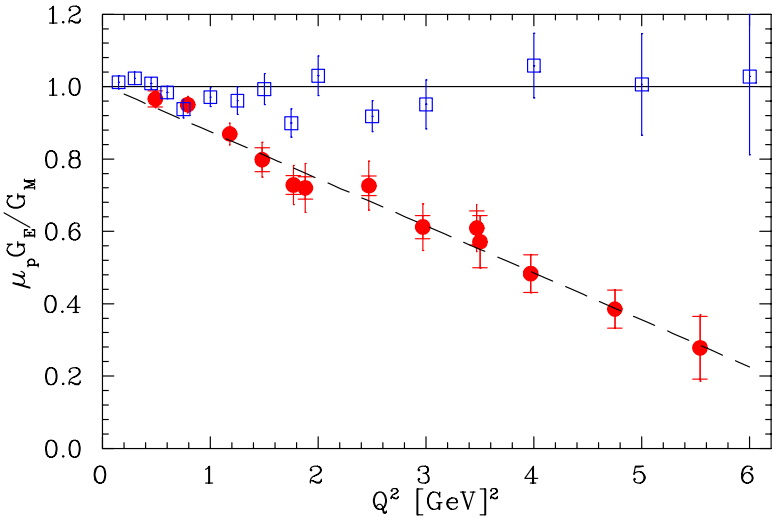

FIG. 1. Ratio of proton electric to magnetic form factor as extracted by Rosenbluth measurements (hollow squares) and from the JLab measurements of recoil polarization (solid circles). The dashed line is the fit to the polarization transfer data.

The form factor ratio $\mu G_E^p/G_M^p$ is shown in Figure 1. The difference between the SLAC Rosenbluth separation data of [2] (see also [3]) and the JLab polarization transfer data of [4] is clear. The question has been whether the difference results from experimental problems, or interesting physics. The questions have largely focused on the Rosenbluth separation experiments, as G_E^p only contributes a few percent to the cross section at high Q^2, and small systematic offsets might lead to large changes in the extracted values of G_E^p. As two recent Jefferson Lab experiments [5] have confirmed the correctness of the SLAC results, attention has shifted instead to physics explanations, in particular to the role of two-photon exchange (TPEX).

The study of the structure of hadrons and nuclei with electromagnetic probes is based on the validity of the one-photon exchange (OPEX) mechanism for electron-hadron scattering, in association with certain radiative corrections. On the basis of this well established formalism, the measured cross sections and polarization observables can be directly related

to the electromagnetic form factors and structure functions. The validity of this approach is based on the assumption that the possible two-photon contribution, where the momentum transfer is shared between two *hard* photons, is small.[1] The relative contribution of the two-photon exchange would be of the order of the fine structure constant $\alpha \simeq 1/137$.

However, even early calculations [6] showed that the simple rule of α counting for the estimation of the relative TPEX to OPEX contributions to elastic eA scattering might not hold at large momentum transfer, due to the steep decrease of the nuclear form factors. In particular, for ed elastic scattering, TPEX might be enhanced already at momentum transfers of the order of 1 $(\mathrm{GeV/c})^2$.

In the case of high Q^2 ep Rosenbluth measurements, the smallness of the contribution of G_E^p to the cross section might make the TPEX correction to G_E^p large. In this case, form factors are arguably not observables that can be extracted from the cross section measurements.

FIG. 2. Two-photon exchange mechanism responsible for single–spin asymmetries in elastic ep scattering. (a) Elastic intermediate state. (b) Inelastic intermediate states.

Figure 2 shows TPEX Feynman diagrams in a hadronic theory. There are two basic contributions to the two-photon exchange which differ by the intermediate hadronic state: the intermediate state is purely elastic, containing only a proton; and the target proton

[1]Standard calculations of radiative corrections for electron-hadron (eh) scattering contain the contribution of TPEX where most of the transferred momentum is carried by one photon, while the other photon has very small momentum.

is excited producing a continuum of particles in the intermediate state. The calculation of diagram (a) is relatively straightforward, but the calculation of diagram (b) is difficult; models with uncertain parameters have to be introduced to describe the coupling to the inelastic states.

The role of TPEX in *eh* scattering was recently revisited in several papers. An analysis of high Q^2 *ed* elastic scattering [7] is suggestive of, but gives no clear evidence for, a TPEX contribution. Measurements of the transverse-polarized beam asymmetry [8,9], which vanishes in one-photon exchange, are clearly nonzero, and exceed theoretical estimates [10]. Even at the low beam energies, below 1 GeV, and four-momentum transfers, about 0.1 – 0.2 $(\mathrm{GeV/c})^2$, the intermediate inelastic states appear to have much larger effect in the data than in theoretical estimates. Thus, it is clear that additional data are needed as constraints if we are to understand the high Q^2 G_E^p discrepancy.

Two theoretical analyzes [1,12] of the differences between the Rosenbluth separation and polarization transfer measurements have been performed. The off-shell intermediate state in TPEX can lead to an ε-dependent correction that distorts the form factors extracted in a Rosenbluth separation. These analyzes indicate that TPEX can reconcile the existing experimental discrepancy, if the TPEX contribution is about 3 – 5 % of the one-photon exchange contribution. This correction is several times the natural α scale, and about as large as the contribution of G_E^p to the cross section.

The TPEX correction is assumed to be essentially linear with ε based on the linearity of the Rosenbluth separation data. But the high Q^2 Rosenbluth separations of [2] rely on renormalizing cross section measured with the SLAC ESA 1.6-GeV spectrometer by a factor of 0.958 ± 0.007, *which ensures the linearity of the Rosenbluth separations.*[2] The

[2]To be precise, the factor is the one derived from the lowest Q^2 point; it was chosen after observing that to ensure linearity one needs the same factor for the five Q^2 at which there were multiple ε points taken with the 8 GeV spectrometer.

renormalization factor, based on the two Q^2, ε points for which there are overlaps of the 1.6 GeV and 8 GeV spectrometers, is 0.953 ± 0.012. The main point is that the data certainly allow few percent nonlinearities over the range of the measurements.

The TPEX correction applies also to the form factors extracted with the recoil polarization technique, but here it changes the form factor ratio and G_E^p by a few percent. Standard radiative corrections are also a few percent and affect the two transfer polarization coefficients similarly, and thus affect the form factor ratio [13] even less.

To summarize, TPEX has been experimentally demonstrated, but there is not as yet a reliable theory of TPEX. The demonstration that TPEX *might* explain the G_E^p discrepancy is certainly not a proof that TPEX *does* explain the discrepancy. For the G_E^p discrepancy to be convincingly resolved, high Q^2 data, in the region of the differing G_E^p measurements, are needed that constrain theories of TPEX. *We propose to measure three observables, the recoil polarization components of the proton, simultaneously - something not possible with any other technique - at a level sensitive enough to determine likely TPEX effects. Furthermore, the measurement can be done in a timely manner with only existing equipment; we do not require large resources to develop new equipment. Finally, by proposing to run with a currently approved experiment, we can save significant installation and overhead times, to help maximize the physics output of Jefferson Lab.*

While the focus of this proposal is obtaining such data, the experimental results have implications beyond simply resolving the discrepancy in the G_E^p measurements. There are several potentially important physics implications of TPEX measurements. For $Q^2 >$ perhaps 2 $(\mathrm{GeV/c})^2$, TPEX probe a combination of generalized parton distributions that are not accessible in other processes [10], providing a unique insight into the structure of the proton. The contributions of TPEX, and more generally loops in quantum mechanics, are important in a number of other processes as well. A better understanding of dealing with hadrons in intermediate-state loops is important for the physics of radiative corrections in extracting strange form factors, meson decays, and hadronic radii, in addition to the electromagnetic form factors.

B. Review of Previous Measurements

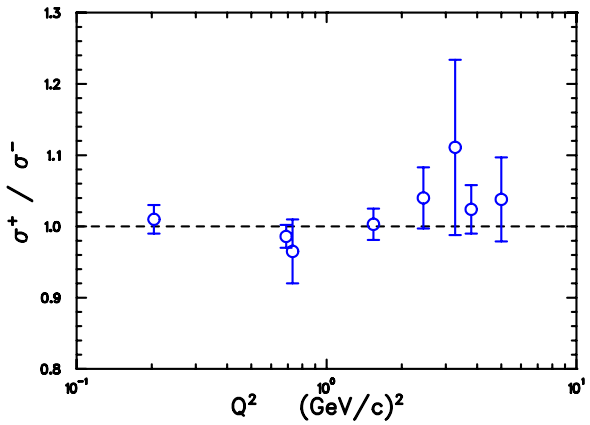

FIG. 3. Some measurements of the ratio $\sigma(e^+p)/\sigma(e^-p)$.

There are several potential measurements that provide a clear signal for TPEX, but few previous measurements have had sufficient precision to obtain a clear signal. The real part of the TPEX amplitude can lead to nonlinearities in the Rosenbluth separation data, or to a modified ε dependence of the polarization transfer data. There is no experimental evidence for either effect. The real part of the TPEX amplitude also leads to an enhancement in the ratio of cross sections $\sigma(e^+p)/\sigma(e^-p)$. If TPEX increases the e^+p cross section by an amount $\delta\sigma$, it decreases the e^-p cross section by the same amount $\delta\sigma$, leading to a ratio of $(\sigma_0 + \delta\sigma)/(\sigma_0 - \delta\sigma)$. The data [14], shown in Figure 3, are not of sufficient precision to provide clear evidence for TPEX – we omit earlier data, which are generally lower in Q^2 and consistent with unity.

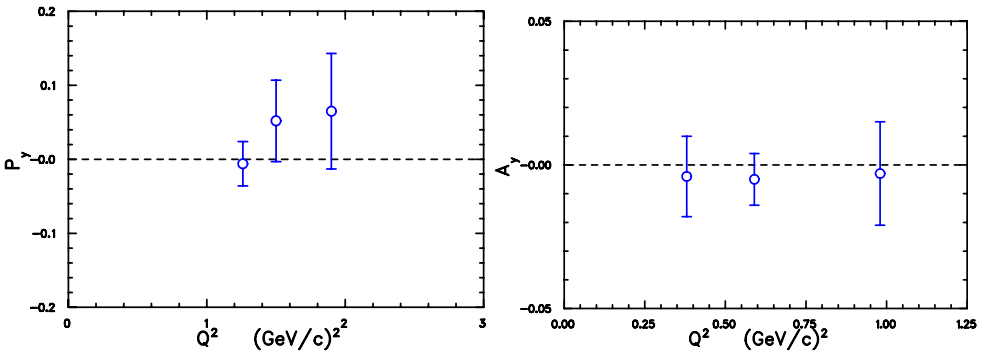

FIG. 4. Left: previous measurements of p_y. Right: previous measurements of A_y.

The imaginary part of the TPEX amplitude leads to single-spin asymmetries. Fig. 4 shows the induced recoil polarization[3] p_y, measured in [15], and the transverse polarized target asymmetry[4] A_y measured in [16]. From the calculation of [10], we expect that $p_y \approx 0.02$ and that $A_y \approx 0.01$ for the various data points shown.[5] The measurements are not sufficiently precise to discriminate between zero and these predictions.

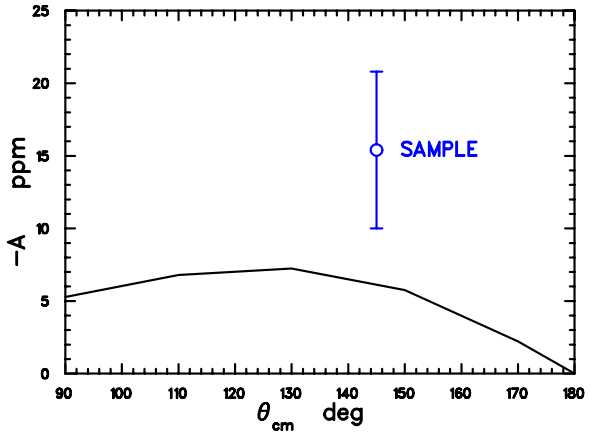

FIG. 5. SAMPLE single-spin beam asymmetry measurement compared to the calculation by Afanasev *et al.* Only the elastic intermediate state contribution is considered in the theory.

TABLE I. Measurements of the single-spin beam asymmetries.

Experiment	Q^2 [(GeV/c)^2]	E [MeV]	θ_e [degree]	A [ppm]
SAMPLE	0.1	200	130 – 170	-15.4 ± 5.4
A4 (preliminary)	0.23	854	30 – 40	-25.3 ± 2.9

[3]We use the following notation for the recoil proton polarization components: p_y normal to reaction plane, P_l rather than $P_{z'}$ along momentum direction, and P_t rather than $P_{x'}$ transverse to momentum and in reaction plane.

[4]From time reversal invariance, $p_y = A_y$ in ep elastic scattering.

[5]Multiple phase conventions are used; so these are sometimes shown with opposite signs.

It is only with recent transverse polarized beam asymmetry measurements that we have unambiguous evidence for TPEX in *ep* elastic scattering. The asymmetries measured by SAMPLE [8] and by Mainz A4 [9] are listed in Table I. Figure 5 shows the SAMPLE result compared to the theoretical calculation of [10]. Only the elastic intermediate state contribution is considered in the theory. Since these are low Q^2 measurements, and the beam asymmetries are independent observables from the hadron asymmetries, these measurements do not bear directly upon the issues of the G_E^p discrepancies - although they can be used to constrain models that predict the G_E^p discrepancies. These measurements are important for experimental systematics, and also provide information useful for calculation of the γZ^0 box diagram.

C. Theoretical Approaches

1. Generalized Formulas

Expressions for the cross section and polarization observables in *ep* elastic scattering are usually presented assuming OPEX. In the general case, neglecting only the electron helicity flip terms due to the small electron mass, the T-matrix of the elastic *ep*-scattering depends on three complex amplitudes, $\tilde{G}_M$ $\tilde{F}_2$ and $\tilde{F}_3$, chosen in [1] as:

$$T = \frac{e^2}{Q^2}\overline{u}(k')u(k)\overline{u}_p(p')\left(\tilde{G}_M\gamma^\mu - \tilde{F}_2\frac{P^\mu}{M} + \tilde{F}_3\frac{\gamma\cdot K P^\mu}{M^2}\right)u(p) \tag{1}$$

In Born approximation, the first two amplitudes, $\tilde{G}_M$ and $\tilde{F}_2$, have the meaning of the G_M and F_2 form-factors which are real functions, while $\tilde{F}_3$ is zero. In the general case, the polarization components of the recoil proton are given by [1]:

$$\begin{aligned} P_t &= -\sqrt{\frac{2\varepsilon(1-\varepsilon)}{\tau}}\frac{C_B(\varepsilon,Q^2)|\tilde{G}_M|^2}{d\sigma} \\ &\quad\times\left\{\frac{|\tilde{G}_M| - \cos\phi_{2M}|\tilde{F}_2|(1+\tau)}{|\tilde{G}_M|} + \frac{\nu\cos\phi_{3M}|\tilde{F}_3|}{M^2|\tilde{G}_M|}\right\} \\ P_l &= \sqrt{(1+\varepsilon)(1-\varepsilon)}\frac{C_B(\varepsilon,Q^2)|\tilde{G}_M|^2}{d\sigma} \end{aligned} \tag{2}$$

$$\times \left\{ 1 + \frac{2\varepsilon}{1+\varepsilon} \cdot \frac{\nu \cos\phi_{3M} |\tilde{F}_3|}{M^2 |\tilde{G}_M|} \right\} \tag{3}$$

All the notations are explained in [1]. Keeping only the terms of order e^2 with respect to the leading one [1]:

$$P_t = -\sqrt{\frac{2\varepsilon(1-\varepsilon)}{\tau}} \frac{|\tilde{G}_M|^2}{d\sigma_{red}} \{R + Y_{2\gamma}\} \tag{4}$$

$$P_l = \sqrt{(1+\varepsilon)(1-\varepsilon)} \frac{|\tilde{G}_M|^2}{d\sigma_{red}} \left\{ 1 + \frac{2\varepsilon}{1+\varepsilon} Y_{2\gamma} \right\} \tag{5}$$

where the reduced cross-section $d\sigma_{red}$ is given by:

$$\frac{d\sigma_{red}}{|\tilde{G}_M|^2} = \frac{d\sigma}{C_B(\varepsilon, Q^2)|\tilde{G}_M|^2} = 1 + \frac{\varepsilon}{\tau} R^2 + 2\varepsilon \left(1 + \frac{R}{\tau}\right) Y_{2\gamma}, \tag{6}$$

and the function $Y_{2\gamma}$ represents the contribution from the two-photon exchange diagrams [6]:

$$Y_{2\gamma}(\varepsilon, Q^2) = \sqrt{\frac{\tau(1+\tau)(1+\varepsilon)}{1-\varepsilon}} \frac{\Re(\tilde{F}_3)}{|\tilde{G}_M|} \tag{7}$$

Here, R is the "true" G_E/G_M form-factor ratio

$$R = \frac{|\tilde{G}_E|}{|\tilde{G}_M|} = \frac{|\tilde{G}_M| - |\tilde{F}_2|(1+\tau)}{|\tilde{G}_M|} \tag{8}$$

The dependence of the amplitudes $\tilde{G}_E$ and $\tilde{G}_M$ on ε is weak [1], of the order of e^2, and therefore they have the meaning of "generalized" form-factors depending only on Q^2. If this is true, the idea of extracting the proton form-factors from ep elastic scattering data survives, although in a more complicated way.

The above formulas connect the two-photon exchange contributions to the cross-section and to the polarizations, i.e. if we know the contribution to the cross-section one can predict the effect on the polarization components. We shall present an analysis from [11] of existing data that uses the formulas given above to extract the TPEX contribution, and then make predictions for the effects on the polarization observables. Important is also that in the

---

[6] The specific ϵ dependence in this formula was first derived in [7].

reduced cross-section $d\sigma_{red}$ and in P_l, the two-photon contribution enters as $\varepsilon Y_{2\gamma}$, while in P_t – only as $Y_{2\gamma}$. That means that if we have a non-zero contribution to the cross-section at small ε, for P_t the two-photon contribution will increase by a factor of $1/\varepsilon$.

2. Hadronic Theories

There have been two basic approaches applied to the hadronic calculations of TPEX. The most obvious approach is to try to explicitly calculate the effect of intermediate elastic and inelastic states [10,12]. The dominance of the Δ resonance suggests that the Δ alone accounts for much of the inelastic contribution – but it should be noted that there are observables in which a Δ dominance approximation clearly fails, such as the magnetic polarizibility of the nucleon. Preliminary calculations [17] indicate that the Δ resonance plays a major role in the large Mainz A4 beam asymmetry measurements, but it only explains about half the observed effect.

Another approach is to approximate the exchange of the two photons by the exchange of axial mesons [18], since the quantum numbers are the same. In this case, TPEX probes an effective axial form factor of the nucleon. Here we summarize the results of the analysis of the data with the axial exchange model.

The positron electron cross-section ratios imply a negative TPEX contribution to the electron cross sections, which is of the form:

$$I_0 = \tau G_M^2 + \epsilon G_E^2 - \delta_1 \sqrt{\tau(1+\tau)}\sqrt{1-\epsilon^2} G_M G_A \tag{9}$$

where G_M, G_E, and G_A are the conventional nucleon magnetic, electric, and axial form factors. Upon adjusting the coefficient δ_1 to the data, the TPEX contribution is typically a few percent. Although the TPEX is inherently nonlinear in the Rosenbluth separations, the nonlinearities are insignificant over the range of the SLAC Rosenbluth data. The axial-exchange corrections to the form factor ratio extracted with the polarization transfer technique are small, a few percent. The axial exchange contribution with the polarization transfer form

factor ratio does not reproduce the Rosenbluth separation data; more TPEX mechanisms are needed, particularly for small ε. As axial-exchange might provide a good phenomenology for medium / long distance physics, it appears that it is also necessary to incorporate additional short-distance physics. It is perhaps not surprising that quark degrees of freedom need to be incorporated at these Q^2.

3. Generalized Parton Distributions

Estimates of TPEX using the generalized parton distribution (GPD) formalism are currently underway. [20] Similar to the case for real Compton scattering, TPEX, or deep doubly-virtual Compton Scattering (DDVCS), depends on form factors that are $1/x$ moments of the GPDs. Transverse polarizations such as p_y are in general related to the absorptive (imaginary), non-forward part of the off-shell Compton amplitude, $\gamma^* p \to \gamma^* p$ scattering; no other process probes this combination of GPDs. At large momentum transfers, perhaps starting from Q^2 above 1 or 2 $(\mathrm{GeV/c})^2$, form factors have been described by model GPDs [21], and TPEX should be described by GPDs as well. Thus, there is the potential for experimental determinations of TPEX to become an important part of efforts to characterize the soft structure of the nucleon at Jefferson Lab.

II. THE PROPOSED EXPERIMENT

A. Strategies for Investigating Two Photon Exchange

As indicated by the discussion above, many observables are indicative of TPEX, including:

1- Measuring the *C-odd* difference between electron-proton and positron–proton scattering cross sections which probes the interference between the real part of the two-photon exchange amplitude with the (real) one-photon exchange amplitude.

2- Analyzing deviations from the Rosenbluth formula – that is, observing a nonlinear behavior as a function of ε – which probes the real part of the interference. Similarly, the beam-target or beam-recoil double-polarization observables can be examined for an ε dependence differing from that in one-photon exchange.

3- Studying *T-odd* parity-conserving single-spin observables - induced polarizations, target asymmetries, or beam asymmetries - which probes the interference between the imaginary part of the two-photon exchange amplitude with the (real) one-photon exchange amplitude.

We propose to measure the ε dependence of all three components of the recoil polarizations at constant Q^2. The advantages of this experiment include:

- The measurements can be done in the high-Q^2 kinematic region in which there is a clear discrepancy between the Rosenbluth and polarization transfer techniques. Thus, there are direct implications for the Rosenbluth and polarization transfer extractions of the proton form factor ratio.

- We will measure polarization transfer (induced polarization) observables sensitive to the real (imaginary) part of the intereference of TPEX with OPEX, with sufficient precision to detect the changes of the size expected from TPEX – we demonstrate this below.

- The polarization transfer observables, in combination with precise cross sections, allow the "generalized" form factors and TPEX to be extracted with a model-independent procedure, outlined in section I C 1, and described further in section III.

- The ratio of polarization transfer coefficients has larger statistical, but smaller systematic, uncertainty as compared to the individual polarization transfer coefficients. It provides an added constraint.

- By measuring at constant Q^2, we keep several aspects of the polarimetry measurement constant, reducing point-to-point uncertainties.
- The experiment requires only equipment that exists, or that will already have been built for other experiments.
- The experiment can be scheduled with Hall C G_E^p-III, resulting in a significant savings of installation and overhead time.

We propose to measure the recoil polarizations with the FPP in Hall C. These measurements will be done at high Q^2, 3.2 (GeV/c)^2. We ask the PAC to endorse our request to be scheduled along with the upcoming Hall C G_E^p-III polarization transfer measurement. The equipment needs of these experiments are identical, so such scheduling would save the several weeks of time needed to reinstall and de-install BIGCAL in Hall C and the HMS FPP, as well as saving some setup / calibration time during the experiment that will be done as part of G_E^p-III. The basic difference between this experiment and G_E^p-III is that we will measure lower Q^2 kinematics than those of the G_E^p experiment, and we will perform more extensive determinations of false asymmetries.

B. Estimating the Size of Two-Photon Exchange

At this point we lack a complete theory for TPEX. In order to make estimates of the size of TPEX effects, we analyze some of the existing Rosenbluth and polarization data to predict the transferred polarization, and we use a model for the induced polarization.

1. Analysis of Existing Data

Our basic assumption here is that the two-photon exchange effects are responsible for the discrepancy between the Rosenbluth and polarization transfer results. We emphasize from the beginning that we will not use any theory or theoretical assumption about the

two-photon exchange contribution except the general formulas of Section I C 1 in which we assume that the two "generalized" form-factors $\tilde{G}_M$ and $\tilde{G}_E$ depend only on Q^2.

Using Eqs.(4,5,6) one can connect the measured cross-sections and polarization component ratio with the unknown "true" form-factor ratio R and two-photon contribution $Y_{2\gamma}$:

$$\frac{d\sigma_{red}(\varepsilon)}{|\tilde{G}_M|^2} = 1 + \frac{\varepsilon}{\tau}R^2 + 2\varepsilon\left(1 + \frac{R}{\tau}\right)Y_{2\gamma}(\varepsilon) \tag{10}$$

$$\frac{P_t}{P_l}(\varepsilon_p) = -\sqrt{\frac{2\varepsilon_p}{\tau(1+\varepsilon_p)}}\ \frac{R + Y_{2\gamma}(\varepsilon_p)}{1 + 2\varepsilon_p Y_{2\gamma}(\varepsilon_p)/(1+\varepsilon_p)} \tag{11}$$

Here ε_p indicates the single value at which we have polarization data, while ε is a variable running over all the values for which there are cross-section measurements. From the above equations one can reconstruct R, and $Y_{2\gamma}(\varepsilon)$ for all ε for which we have cross-section data. The problem is, however, that the "generalized" magnetic form-factor, which enters in the normalization of the reduced cross-section in the above formula, is unknown. Therefore, by scaling the reduced cross-section one can produce the whole spectra of possible solutions for R and $Y_{2\gamma}(\varepsilon)$ that are consistent with the existing data.

The procedure described above is demonstrated in Fig.6 (taken from [11]) using the cross-section data at $Q^2 = 3.25$ GeV^2 [2] and polarization results [4] interpolated to the same Q^2 value. One can see that if $Y_{2\gamma}(\varepsilon)$ is negative, there are significant two-photon exchange effects at small ε. This follows directly (i) from the approximate linearity of the Rosenbluth data, and (ii) from the specific structure of the two-photon exchange contribution to the polarization components and cross-section Eq.(4, 5, 6) as discussed above. The theoretical calculations [12] of the TPEX contribution to the cross-section are transformed (Fig.6) to $Y_{2\gamma}(\varepsilon)$ using a similar procedure as for the cross-section data. These calculations also indicate visible effects at small ε.

Although in the example above we have used only the data of [2] for the cross-section, other recent Rosenbluth measurements [3,22] confirm the approximate linearity of the reduced cross-section as function of ε. The fits of the data sets in Fig. 6 were intentionally extended down to $\varepsilon = 0.13$ which corresponds to the lowest ε point of the Super-Rosenbluth experiment [3]. The results [5] are not yet published, but the cross-section data are consis-

tent with a linear function, suggesting the data points will be at the lower end of the solid curves in Fig. 6.

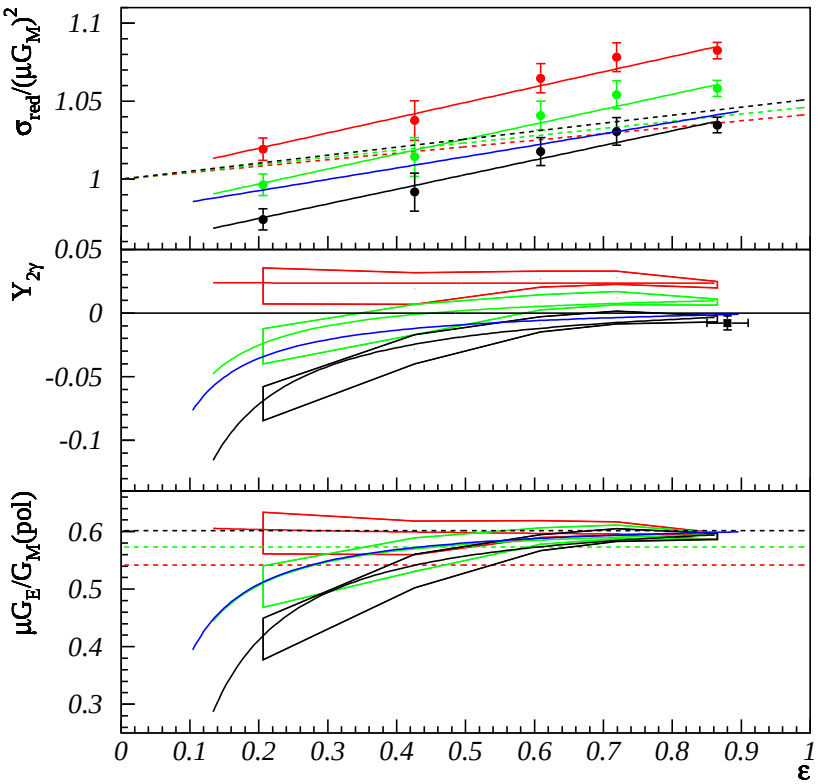

FIG. 6. Analysis of TPEX at $Q^2 = 3.25$ GeV^2. Top panel: data points - the reduced cross-section [2], the data are normalized by three equidistant values of the G_M to demonstrate the variations of the reconstructed quantities. Middle and bottom panels: The black, green and red colored areas are the solutions of Eqs.(10,11) for the two-photon contribution $Y_{2\gamma}$ (middle) and the form-factor ratio calculated from the transferred polarizations in Born approximation (bottom), reconstructed from the polarization results [4] and from the same-color cross-section data set in the top panel. The black, red, and green solid curves in all panels are from fits to the cross-section data points. The data point at $\varepsilon = 0.88$ in the middle panel is from e^+/e^- cross-section ratio measurements [14] (see text). The blue solid curves in all panels are from the calculation [12] of the TPEX cross-section corrections (see text). The dashed curves in the top panel are the Born approximation ($Y_{2\gamma} = 0$, no TPEX) cross sections that correspond to the same color solid curves. The dashed curves in the bottom panel give the corresponding true form-factor ratio R, rather than the Born ratio.

The e^+p to e^-p cross-section ratio measurements [14] imply additional constraints [23] on the two-photon contribution. If the two-photon exchange correction $Y_{2\gamma}(\varepsilon)$ is positive it increases the electron-proton cross-section and decreases the positron-proton one. The average cross-section ratio measured for $Q^2 > 2$ (GeV/c)^2 at high ε is 1.034 ± 0.024 [14] (see Fig. 3), which corresponds to the $Y_{2\gamma}(\varepsilon)$ data point as shown at the middle panel in Fig.6. This data point certainly rules out positive TPEX contribution at high ε. Since $Y_{2\gamma}$ falls monotonically as ε decreases (see Fig. 6) positive $Y_{2\gamma}$ values at middle and low ε region are also excluded.

From this analysis we conclude that based on the general formulas given by [1] and on the existing data, we expect significant two-photon exchange effects at low ε.

2. Induced Polarization

Calculations of p_y in *ep* elastic scattering, from [10], are shown in Figure 7. (There are also calculations in [19], which consider only the intermediate elastic state.) The induced polarization is proportional to a kinematic factor of $\sin\theta_{\rm cm}$, so it is important not to measure too near 0° or 180°.[7] For energies of 1, 2, 4, and 6 GeV, the estimated peak asymmetries are about 1.1, 1.8, 2.3, and 2.5%, at electron c.m. angles of 100°, 80°, 70°, and 60°. The estimated polarization remains significantly large over about half of the angular range.

---

[7] At 0° or 180° the transverse direction is undefined, so both p_y and the transferred x component of polarization vanish.

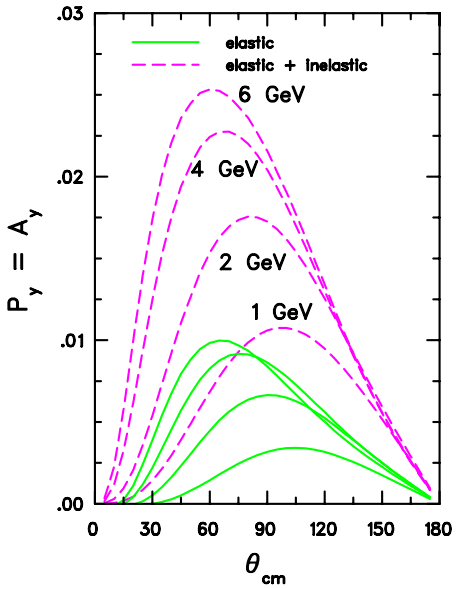

FIG. 7. Proton induced vector polarization component, p_y, as a function of the electron $\theta_{\rm cm}$ scattering angle for different beam energies. The dash (solid) line shows the total (elastic only) TPEX effect.

In the calculations of [10], the polarization arises about equally from elastic and inelastic contributions. Since resolving the difference between Rosenbluth and polarization transfer techniques appears to require somewhat larger than expected TPEX, and since the Mainz beam asymmetry measurements are significantly larger than TPEX estimates, it is quite possible that p_y is larger than these predictions. However, it cannot be very large, above about 5 %, or it would have been seen in earlier SLAC p_y and earlier JLab G_E^p measurements.

C. Experimental Technique

We propose to use BIGCAL, the large electron calorimeter being built initially for E01-109, G_E^p-III in Hall C, in coincidence with the HMS arm equipped with a polarimeter in Hall C. Determining *ep* coincidences with this technique is standard; it was demonstrated in the G_E^p-II experiment [4] in Hall A for Q^2 from about 3 to 6 (GeV/c)^2. The purpose of BIGCAL is to reduce background by ensuring exclusivity of the reaction. This is important especially for the low ε points where the single arm background is significant. The distance

from the calorimeter to the target needed to match the HMS acceptance is similar to the distances for E01-109.

All information for the polarization analysis is determined by detectors in the magnetic spectrometer. Since the viability of the coincidence measurements has been experimentally demonstrated, we will not discuss them further; the discussion will focus instead on polarimetry.

D. Polarimetry Systematics

These polarization measurements are insensitive to all off the usual systematic issues that affect cross section measurements, such as measuring beam current, target thickness, and solid angle. The experimental issues with polarimetry include: knowing the beam polarization, understanding spin transport in the spectrometer, knowing the FPP analyzing power, and understanding the FPP false asymmetries. It is important to note that, for an ε dependence at constant Q^2, the protons are measured at the same energy for all kinematic points, so there is no change in leading order to the spectrometer spin transport, to the FPP analyzing power, or to the false asymmetries.[8] Thus, relative polarizations will have small systematic uncertainties.

The FPP analyzing power is needed to determine absolute polarizations. In OPEX, each of the two polarization transfer components depends only on the ratio G_E/G_M, and the two components can be used to extract the analyzing power as well as the form factor ratio.[9] The

---

[8]There is a small higher order correction, as the change in cross section and momentum with scattering angle varies slightly between the different ε points, leading to slightly different distributions of focal plane events.

[9]The model-independent analysis of [11] indicates that the extraction of the analyzing power is insensitive to the TPEX; corrections are a few percent at most. This will be discussed further below.

form factor ratio (analyzing power) is more sensitive to P_t (P_l). Considering the helicity-dependent azimuthal asymmetry directly measured in the polarimeter, the form factor ratio (analyzing power) depends on the phase (magnitude) of the azimuthal asymmetry distribution. The absolute uncertainty on the analyzing power will be 2 – 3 % from statistics of the calibration, spin transport uncertainties, and knowledge of the beam polarization. This is insignificant for the total uncertainty budget of the experiment. More importantly, the point-to-point uncertainty in the analyzing power is negligibly small, since all measurements are done at the same proton energy.

The beam polarization is measured with a Møller polarimeter. The Hall C polarimeter uses a large, 4 Tesla field to fix the analyzing foil polarization. This leads to a beam polarization uncertainty of $\approx$ 1 %. The beam polarization is measured in all kinematic points to determine the polarization transfers. Over "short" periods of time, during which there is stable accelerator operation, beam polarization has been measured to be stable to a few tenths of a percent. Over "long" periods of time, polarization changes of $\approx$ 1.5 % can be seen; some of these reflect actual changes in beam polarization (different amounts of bleed through of beam of other halls, different spot on photocathode, ...) while others appear to reflect systematic uncertainties in the polarimeter (different focus of beam into polarimeter, ...). The statistical uncertainty in P_t (P_l) will be about about 5 % (0.5 %) relative. Thus, it is necessary to monitor the beam polarization carefully, particularly if there are accelerator changes, so that the uncertainties on P_l do not increase.

The spin transport of the HMS spectrometer will be thoroughly investigated as part of the G_E^p-III commissioning. HMS is a well calibrated spectrometer; particle distributions are well modeled by existing Monte Carlo simulations. The elements of this investigation, as performed in Hall A, include studying the simulations of the focal plane distributions vs. data, examining the variation in focal plane spin across the focal plane, and studying the effect on the distributions of varying quadrupole fields away from nominal settings.

The basic technique to zero out false asymmetries with the polarimeter is to use a combination of cosmic ray data and straight-through data, taken with the analyzer removed,

to align the detectors. We have increased the phase space probed in the alignments in Hall A by using a carbon diffuser after the VDCs to scatter particles into a larger area within the focal plane. Once the alignment is done, no real tests of false asymmetries have been performed in previous experiments, as it is difficult to obtain a clean sample of unpolarized protons, and as it was not needed for the polarization transfer data. The false asymmetries cancel in the polarization transfer measurements, as the proton spin flips with beam helicity, but false asymmetries are helicity independent. Thus, it was not possible to justify the beam time needed to calibrate out the false asymmetries in our high precision G_E^p measurements in Hall A, and the elastic *ep* measurement was used to determine false asymmetries for other lower precision experiments.[10]

The false asymmetries are however crucial for the induced polarization measurements of this experiment. In the following paragraphs, we discuss three techniques we will use to measure and control the false asymmetries in this experiment so that the induced polarization can be reliably extracted. The three techniques provide redundant independent measurements of the false asymmetries.

First, we use the lowest ε point of the proposed ε dependence to provide protons with a nearly vanishing induced polarization, based on the calculations of [10]. These protons illuminate essentially the same phase space of the polarimeter as the intermediate ε points. Thus, they provide a measurement of the false asymmetry.

The second measurement is one with the proton induced polarization rotated through spin precession to be approximately longitudinal. The longitudinal component leads to

---

[10]These observations explain why it is essentially impossible to analyze the existing Hall A FPP data for induced polarizations. Under the assumptions that the false asymmetries are constant, independent of time, proton energy, and particle distribution in the focal plane, we could analyze the existing data to produce a low statistics, possibly 1-2 σ (statistical) result, that no person familiar with polarimetry analysis would take very seriously.

no asymmetry in the polarimeter, and cleanly checks the quality of the false asymmetry calibration. With the 25° central bend angle of HMS, this 90° precession spin transport hole occurs at $Q^2 = 1.775$ (GeV/c)^2.

The third test is to measure the false asymmetries with the $ep \to e'\pi^+ n$ reaction. The use of a coincidence measurement, while not strictly necessary, ensures a clean sample of π^+. This reaction has the benefit that large π^+ rates are possible, and there are no spin effects from the spin-0 pion. For 1 – 2 GeV/c p and π^+, the pp and pA cross sections are about 20 % larger than the corresponding $\pi^+ p$ and $\pi^+ A$ cross sections, and all cross sections are largely inelastic. Thus there will be similar absorption effects for protons and pions in the analyzer. Note that differential absorption depending on scattering angle is not an issue for particles normally incident on the face of the analyzer. To optimize uncertainties, the π^+ calibrations need to be run for statistics about equal to those of the ep measurements. Multiple measurements will be made to check for consistency and time dependences.[11]

A fourth technique was suggested in the PAC review of our letter of intent LOI 03-101: the PAC suggested measuring the same induced polarization on both sides of the beam, scattering left and scattering right. In a spectrometer fixed reference frame, the induced polarization changes sign, pointing "up" on one side of the beam, and "down" on the other side. Unfortunately, such measurements are not possible in Hall C, with HMS restricted to beam right. (Even in Hall A, switching the Hall A hadron detectors for G_E^p-II in late 2000 required about one month of down time; moving one HRS spectrometer to the other side of the beam line requires de-constructing and reconstructing the beam line in Hall A, and would have to be undone afterward.) One solution would be to repeat a kinematics of this proposal in a subsequent experiment in Hall A - Hall C HMS is beam right, whereas the

---

[11] To ensure that the π^+ measure the false asymmetries well, it is necessary to check chamber efficiency plateaus for π^+. The π^+ have smaller dE/dx than protons and, if signals are close to discriminator threshold levels, the π^+ might have different false asymmetries than do the protons.

Hall A FPP is now beam left. We do not request this measurement at this time.

E. Kinematics

The choice of kinematics involves a trade off between high Q^2, for which TPEX is relatively larger, and the difference between Rosenbluth and polarization transfer techniques are large and increasing, and low Q^2, for which experimental uncertainties are smaller. We choose $Q^2 = 3.2$ (GeV/c)^2, to overlap previous, high-precision, cross-section measurements. The choice of ε points depends upon several considerations. Although we have given arguments that significant TPEX effects are expected at low ε region, it is important to cover a wide range of ε. The points should be at ε for which there are precise cross sections. This is very important for testing the consistency of the results and reconstruction of the "generalized" form-factors as discussed later. The calorimeter, while it enhances the experiment by allowing matching of solid angles, is not trivial to move in Hall C: it requires several hours to crane the calorimeter into position for each setting, and the rails on the floor of Hall C do not allow the calorimeter to be put in arbitrary locations. This suggest fewer, higher precision, ε settings. The range of angles is limited in Hall C; the maximum calorimeter angle will likely be $\theta_{\rm lab} \approx 105^\circ$. For constant Q^2 kinematics, each ε point requires a different beam energy and spectrometer angles. The proposed kinematic points are shown in Table II.

TABLE II. Kinematics for $Q^2 = 3.2$ (GeV/c)^2.

Q^2 (GeV/c)^2	E (GeV)	ε	θ_e (deg)	p_e (GeV/c)	θ_e (deg, cm)	θ_p (deg)	p_p (GeV/c)
3.2	2.2624	0.131	105.632	0.5571	145.095	12.538	2.4714
3.2	2.8416	0.443	59.704	1.1363	113.477	23.390	2.4714
3.2	3.7713	0.696	37.377	2.0661	90.963	30.497	2.4714
3.2	4.7003	0.813	27.583	2.9950	78.347	34.134	2.4714

F. Time Request

In this section we detail our time request, including time for calibration data. The time estimates assume 75 μA of 80 % polarized beam, and use the figure of merit from the carbon analyzer of the G_E^p-I experiment.

Our first request is for the data points at four ε settings. Each point requires 4 days for the data taking. We request 2 additional days for overhead, needed to position the calorimeter and take Møller measurements. The total time for these settings is 18 days.

The first calibration request is for time to measure an ep elastic data point at $Q^2 = 1.775$ (GeV/c)^2. The central spin precession angle for these kinematics is $\chi = 90°$. The best kinematics, to overlap a beam energy of the data and nearly match calorimter angles, is 2.8416 GeV beam energy, with scattering angles $\theta_e = 39.64°$, $\theta_{e\,cm} = 77°$, and $\theta_p = 39.6°$. This is the beam energy of the $\varepsilon = 0.443$ data point, and nearly matches the 37.4° calorimater angle of the $\varepsilon = 0.696$ data point. Hence p_y, which is estimated to be about 0.02, is rotated to be essentially longitudinal, and the false asymmetry will be directly measured with protons. A 1-day measurement corresponds to a false polarization uncertainty of about 0.004, which is adequate for the systematics of our data. We request four days, so that we may study the variation in the physics plus false asymmetry across the focal plane. Since the physics is not changing, a constant false asymmetry leads to a linear variation in the asymmetry, better calibrating the polarimeter and allowing the induced polarization to be reliably extracted. Despite the unfavorable spin transport, the estimated uncertainty on p_y is about 0.008, for a 3σ measurement. To summarize, we request four days for this false asymmetry measurement.

Our second calibration request is for measurements of the $p(e, e'\pi^+)X$ reaction, to use pions to calibrate the polarimeter. We estimate that the pion data can be taken at kHz rates, about 3 – 4 times the rate of the ep coincidence data. Thus, matching the statistical uncertainties of the ep data requires only 1 day of pion measurements. To check on any time dependence to the systematics, we wish to repeat the measurement 3 times. Thus, we

request 3 days for three pion measurements.

In summary, we request 18 days to do a four-point ε dependence of the recoil polarizations. We request 4 days to perform a false asymmetry calibration measurement at $Q^2 = 1.775$ (GeV/c)^2. We request 3 days to perform false asymmetry calibrations with pions. The 25 days are sufficient for this experiment; no additional time is needed, assuming that it is scheduled to run with G_E^p-III, E01-109, in Hall C.

This beam time request leads to the estimated polarizations and uncertainties shown in Table III. Here the polarization transfer numbers assume OPEX, while the induced polarization numbers are based on the calculations of [10], and are the same as shown in Fig. 8. Uncertainties are based on the time estimates detailed in Section II F. We obtain significant measurements of all three recoil polarization components, with several σ deviations from 0 for p_y and better than 4% measurements of the form factor ratio.

TABLE III. Expected polarization observables (and estimated statistical uncertainties) for $Q^2 = 3.2$ (GeV/c)^2.

ε	P_t	p_y	P_l
0.131	-0.1058 (0.0035)	0.0033 (0.0039)	0.9850 (0.0049)
0.4443	-0.1533 (0.0037)	0.0128 (0.0039)	0.8772 (0.0052)
0.696	-0.1403 (0.0038)	0.0199 (0.0038)	0.6940 (0.0053)
0.813	-0.1182 (0.0038)	0.0230 (0.0037)	0.5596 (0.0053)

G. Expected Results: Induced Polarization

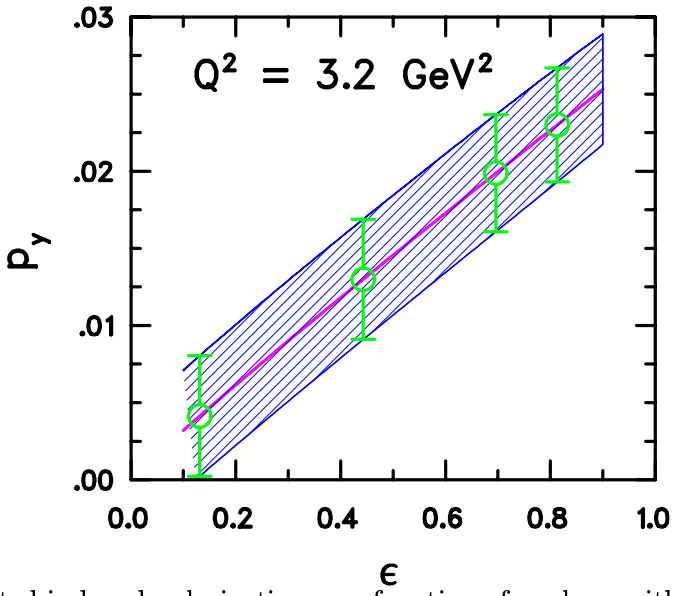

FIG. 8. The estimated induced polarization as a function of ε, along with statistical uncertainty bands assuming 4 days of beam time at each point.

Figure 8 shows the expected results for the induced polarization. The values use the calculation of Afanasev, Akusevich, and Merenkov [10]. On the basis of the calculation and the statistical uncertainties, the high ε point will be several σ from zero. This measurement is clearly sufficient to determine whether or not the induced polarization is anomalously large, as might be expected from the inelastic enhancement of the Mainz A4 beam asymmetry. The false asymmetries will be determined with similar statistical uncertainty as the measurements shown here. Depending on the variation of the various false asymmetry measurements, this systematic uncertainty could be somewhat smaller than the statistical uncertainty shown. The approximate constancy of the experimental uncertainty with ε results from matching the solid angle of the calorimeter to the solid angle of HMS, which keeps the count rate fairly constant, in contrast with single arm (e, e').

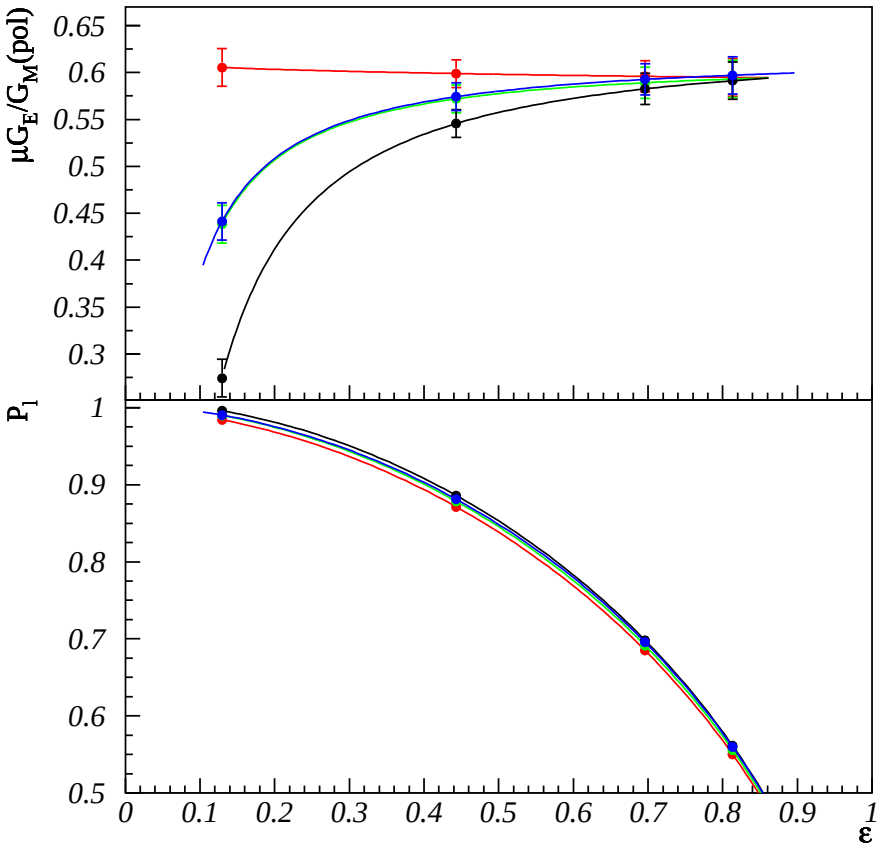

FIG. 9. Estimated form factor ratio in Born approximation, proportional to P_t/P_l (top), and longitudinal polarization P_l (bottom) - data points sitting on different curves that correspond by color to Fig.6.

The expected results for the transferred polarization are demonstrated in Fig.9. Instead of showing the polarization ratio P_t/P_l we plot the form-factor ratio in Born approximation which is proportional to P_t/P_l. In contrast to the longitudinal polarization, the transverse component is very sensitive to the TPEX contribution as discussed above. Only the statistical errors are given. The systematic uncertainties will be discussed in connection with the reconstructed amplitudes in the next section.

I. Reconstruction of the "Generalized" Form-Factors

In this section we discuss a procedure for a reconstruction of the real parts of the *ep*-elastic amplitudes $\tilde{G}_M$, $\tilde{F}_2$, and $\tilde{F}_3$ as defined in Section I C 1, and called here also "generalized" form-factors. We will use the TPEX formulas Eqs.(4-8) that connect the three observables, two polarization components and the cross-section, with the three unknown quantities $|\tilde{G}_M|$, $|\tilde{F}_2|$, and $\Re(\tilde{F}_3)$. Because the imaginary parts of $\tilde{G}_M$ and $\tilde{F}_2$ are negligible [1] we associate $|\tilde{G}_M|$ and $|\tilde{F}_2|$ with their real parts, although this is not needed for the analyses. We will estimate the uncertainties that one can achieve in reconstructing these quantities based on the proposed kinematics and beam time request (shown before in subsections II E and II F). The most important part of the proposed investigations is to determine whether we are really measuring form-factors, i.e. amplitudes that depend only on one variable. Several ways of testing the ε independance of the "generalized" form-factors will be demonstrated. All the analyzes and figures are taken from [11].

Using the Focal Plane Polarimeter, the asymmetries hA_yP_t and hA_yP_l are actually measured, where A_y is the analyzing power of the polarimeter, and h - the beam helicity. Since Q^2 and hence, the proton momentum is fixed, the analyzing power A_y is the same for all the measurements. This means that the polarization component ratio $P_t/P_l(\varepsilon)$ and the ratio of the longitudinal components at two different ε values: $P_l(\varepsilon_1)/P_l(\varepsilon_2)$ can be measured with very high precision, since A_y cancels out. The uncertainties in the spin transport (although not dominant) from the target to the focal plane where the polarizations are being measured, cancel out in the $P_l(\varepsilon_1)/P_l(\varepsilon_2)$ ratio. As for the beam helicity h, it also cancels out in the P_t/P_l ratios, and we assume 1% error for the ratio of the helicities at the two ε values, $h(\varepsilon_1)/h(\varepsilon_2)$, that will affect only the $P_l(\varepsilon_1)/P_l(\varepsilon_2)$ ratio. The kinematics (subsection II E) are chosen to be the same as in the Super-Rosenbluth experiment (E01-001) so that we can use their high-precision cross-section measurements.

Thus, for each ε value we will have three measured quantities P_t, P_l, and $d\sigma$, that depend (Eq.(4, 5, 6)) on the "generalized" form-factor ratio $R = |\tilde{G}_E|/|\tilde{G}_M|$, magnetic form-factor

$|\tilde{G}_M|$, and the two-photon contribution $Y_{2\gamma} \sim \Re(\tilde{F}_3)/|\tilde{G}_M|$, all being combinations of the real parts of the three reaction amplitudes and therefore, generally, functions of both Q^2 and ε. The analyzing power A_y is known only with poor precision, therefore we consider it as unknown.

As discussed above, the dependence of the amplitudes $\tilde{G}_E$ and $\tilde{G}_M$ on ε is weak [1]. In the next subsections we will make successively different assumptions about this dependence, starting from the most restrictive case, that $\tilde{G}_E$ and $\tilde{G}_M$ are functions only of Q^2 and going to the most general case. We will not make any assumptions about the two-photon contribution $Y_{2\gamma}$.

Since we have measurements at several ε values, except for the most general case, we have an overdetermined system of equations, and it is obvious that all the physics quantities can be determined. In order to understand the sensitivity of the reconstructed amplitudes to the measured quantities, we found it very informative to demonstrate the procedure graphically. For this purpose, from Eqs.(4, 5, 6) we represent the three unknowns $|\tilde{G}_M|$, $Y_{2\gamma}$, and A_y as functions of the fourth one, R. These functions are ratios of polynomials with coefficients that depend on ε and on measured quantities: A_y depends on P_l and P_t/P_l, $|\tilde{G}_M|$ on $d\sigma$ and P_t/P_l, and $Y_{2\gamma}$ on P_t/P_l. These functions are demonstrated at Fig. 10 and Fig. 13 (discussed later) for each ε separately. The widths represent the experimental uncertainties. The estimations of the statistical uncertainties are based on the assumptions discussed in subsection II E. The width of A_y includes also a 1% systematic uncertainty of the beam helicity. We have used 0.8% point to point uncertainties for the cross-sections as stated in the preliminary results of the Super-Rosenbluth experiment [3]. The overall systematic error of about $4-5\%$ [3] is not included, but it affects only the absolute value of the magnetic form-factor as reconstructed below.

We assume that R and $|\tilde{G}_M|$ depend only on Q^2. Graphically that means that the functions plotted in Fig. 13 for each ε separately, can be put together as shown at Fig. 10. One can see that the form-factor ratio R can be reconstructed by finding the common crossing point of the $|\tilde{G}_M|(R)$ functions at different ε values (top panel), or, similarly, using the $A_y(R)$ functions (bottom panel). Because of the high precision cross-section measurements, the former method gives smaller uncertainties, while the uncertainties in the latter method, discussed in the next subsection, are limited mainly by the beam helicity uncertainty.

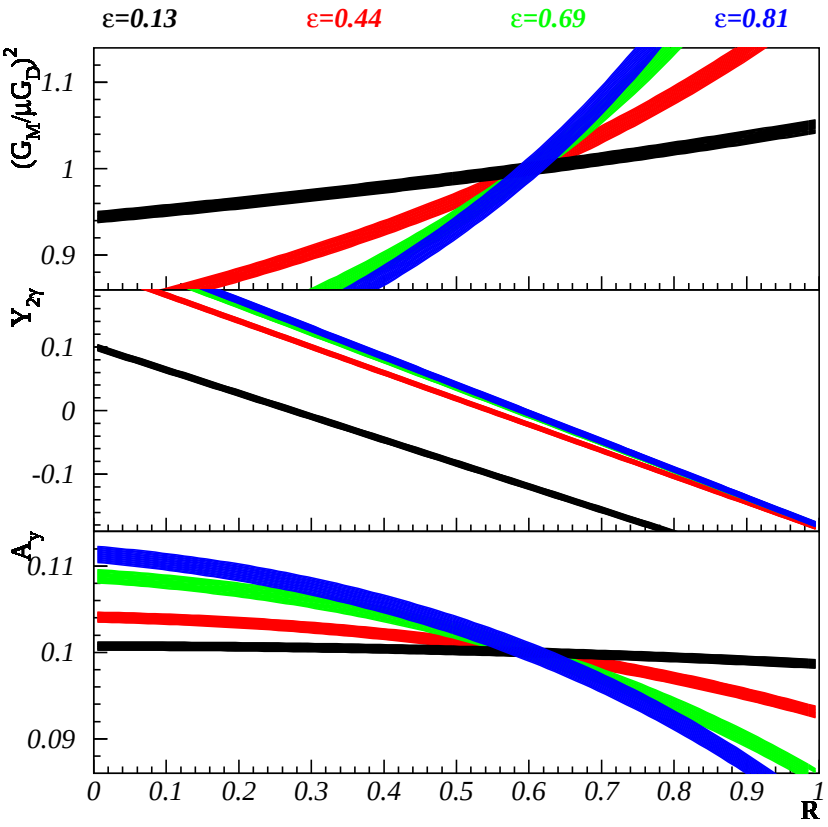

FIG. 10. Graphic solution of Eqs.(4, 5, 6): squared normalized magnetic form factor G_M, two-photon exchange term $Y_2\gamma$, and analyzing power A_y as a function of "generalized" form-factor ratio R. The widths represent the statistical and systematic errors due to uncertainties in P_t/P_l, P_l and $d\sigma$. Different colors correspond to different ε values.

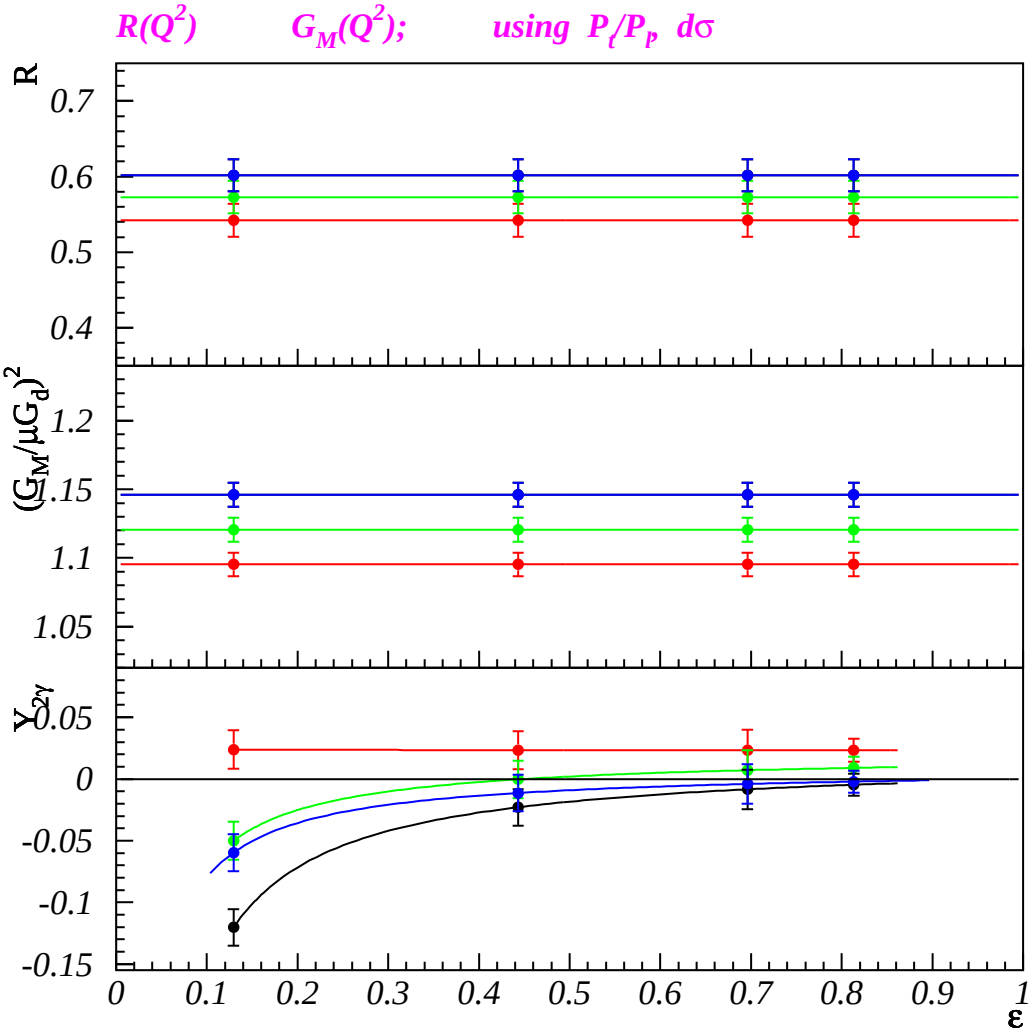

FIG. 11. Estimated uncertainties of the reconstructed "generalized" form-factor ratio R, squared normalized magnetic form-factor G_M and two-photon exchange term $Y_2\gamma$ – the data points sit on different lines that correspond by color to Fig. 6. This analysis assumes R and G_M do not depend on ε.

Thus, using only the polarization ratio and cross-section measurements one can reconstruct the "generalized" form-factor ratio and magnetic form-factor from the crossing point at the top panel in Fig. 10, and then form the $Y_{2\gamma}(R)$ dependence for each ε separately – the two-photon contribution. The estimated uncertainties for the reconstructed quantities are shown in Fig. 11 for the different two-photon contributions as used in Fig. 6. The figure

demonstrates that under the above assumptions one can achieve high precision results for the form-factors and for the ε dependence of the two-photon contribution.

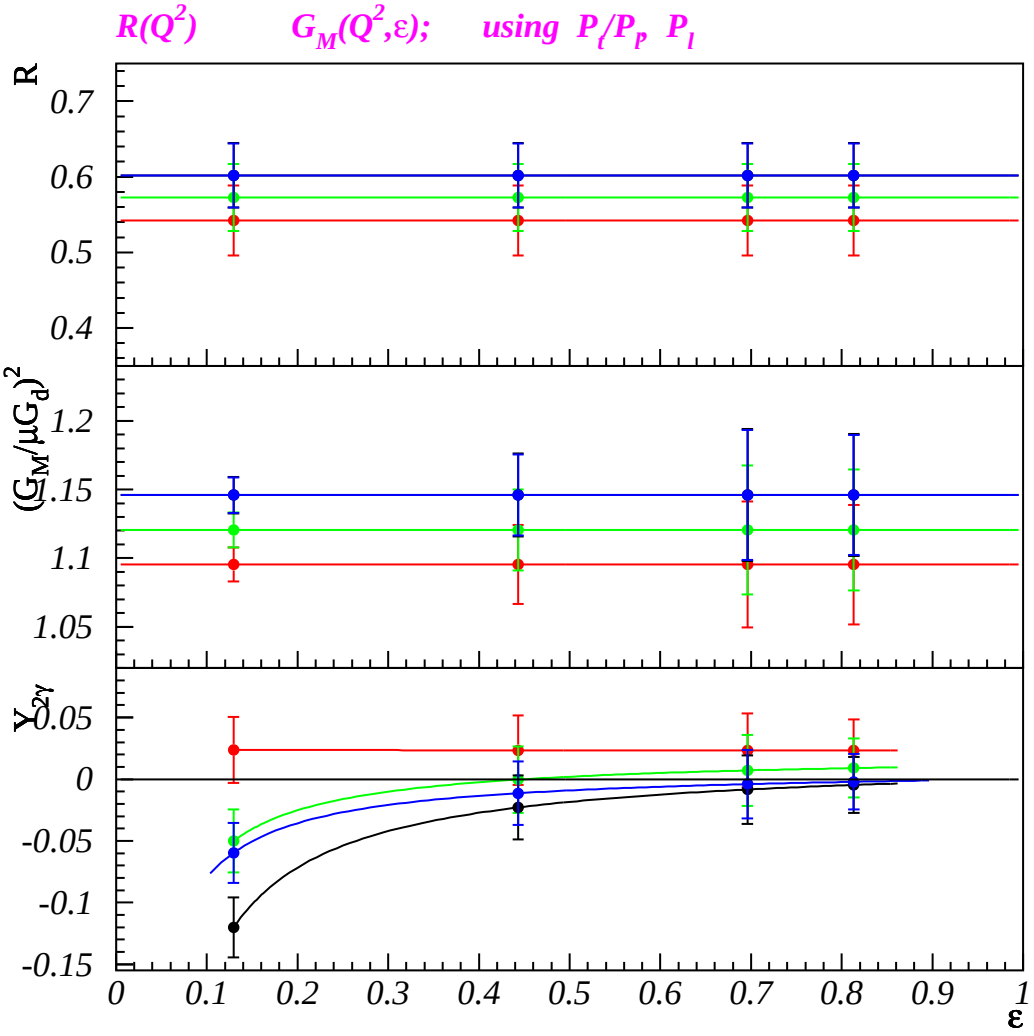

FIG. 12. Same as Fig. 11 but assuming only R does not depend on ε.

2. Reconstruction of the "generalized" form-factors assuming their ratio is ε independent

Now we assume R depends only on Q^2 but $|\tilde{G}_M|$ may depend also on ε. In this case, one can reconstruct R by finding the crossing point of the $A_y(R)$ functions for different ε (Fig. 10 bottom panel) since R and A_y do not depend on ε. Then, using the $|\tilde{G}_M|(R)$ and $Y_{2\gamma}(R)$ dependences for each ε separately, one can reconstruct $Y_{2\gamma}$ and $|\tilde{G}_M|$ as functions of

ε.

The results of such procedure are shown at Fig. 12. The precision is worse than in the previous case mainly for two reasons: (i) poorer A_y precision limited by the beam helicity uncertainty (1%) and statistics (0.5 - 1% for different ε), and (ii) less sensitivity to R as seen by comparing the relative slopes of the $A_y(R)$ and $|\tilde{G}_M|(R)$ functions at different ε (Fig. 10). Nevertheless, the number of factors that affect the systematics is much smaller for P_l measurements than for cross-section measurements, so it is always worth using both methods to check the consistency of the results. In fact the proposed measurements will provide the first constraints on the real parts of the amplitudes that are independent of existing cross section data.

3. Testing ε independence of the "generalized" form-factor

One way to test the ε independence is to compare the results for R obtained by using the $|\tilde{G}_M|(R)$ crossing (subsection III1) and $A_y(R)$ crossing (subsection III2) (top and bottom of Fig. 10). Any inconsistency of the results might indicate an ε dependence of R, $\tilde{G}_M$ or both. Assuming R is ε independent as in the previous subsection, an ε dependence of $\tilde{G}_M$ at a level of 1 to 5% can be identified (see Fig. 12).

The second way is to check for the common crossing point of the four curves $|\tilde{G}_M|(R)$ at the top panel of Fig. 10. Again, any inconsistency, taking into account the experimental uncertainties represented by the widths of the curves, may indicate R and/or $\tilde{G}_M$ ε dependence. Disagreement of $5-10\%$ for R can be identified with this method.

The third way is to check for the common crossing point of the $A_y(R)$ curves at the bottom panel of Fig. 10. Since A_y is the same for all ε the reason for inconsistency must be the ε-dependence of R, which however can only be identified at $10-20\%$ level.

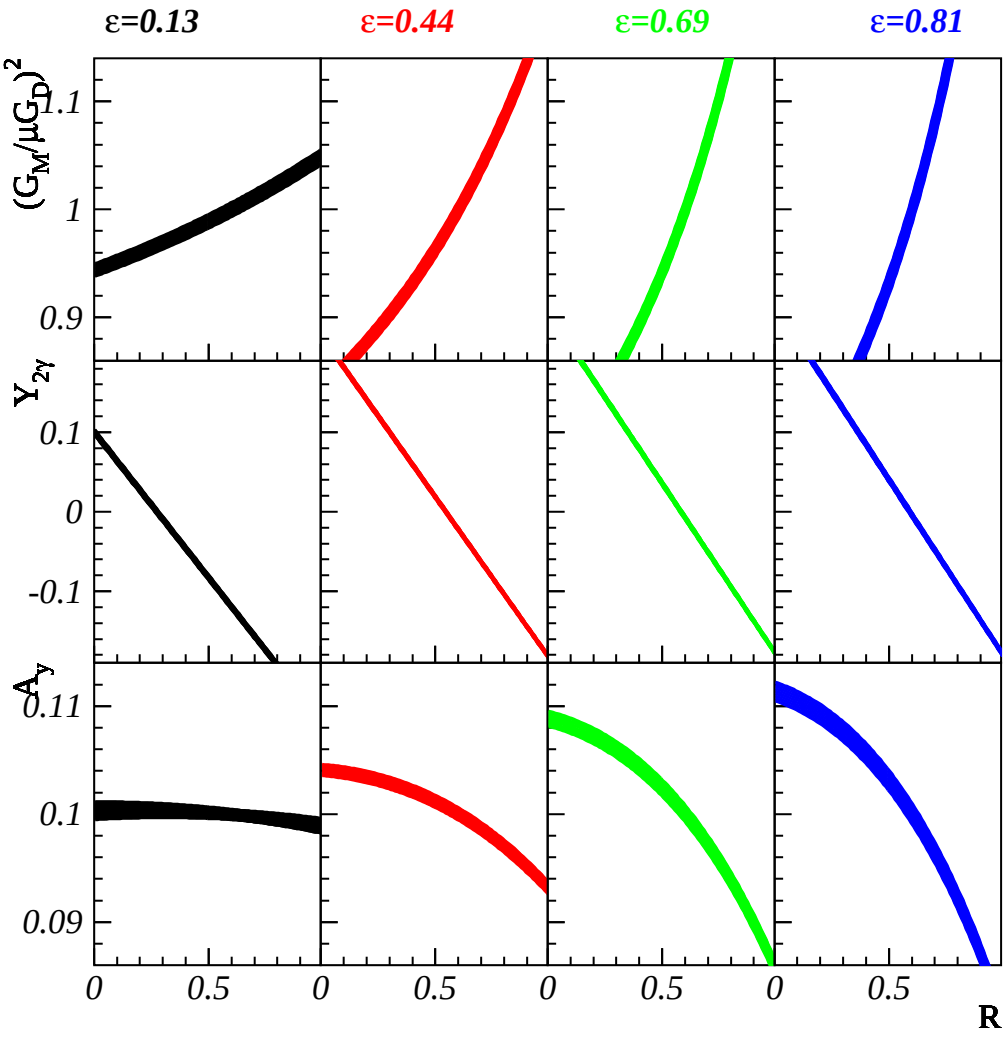

FIG. 13. Same as Fig. 10 but each ε value shown in different column. The width of A_y for $\varepsilon = 0.13$ represents also the model uncertainties as shown in Fig. 6.

Finally, the fourth way for testing the ε independence is to attempt to reconstruct all the three amplitudes allowing all of them to depend on ε. In this case we have 13 unknowns (three amplitudes for each ε point and A_y) and 12 equations (three for each point). Fortunately, the longitudinal polarization component P_l at low ε is defined mainly by kinematic factors and must be identical to 1 at the limit $\varepsilon = 0$. Therefore, the dependence of A_y on R for the lowest ε point is very weak as demonstrated in the bottom left box in Fig. 13. The width there indicates not only the statistical and systematic uncertainties but also the model

dependence of the result by using all different two-photon contributions as shown at Fig. 6. As a result, assuming only a wide range of the form-factor ratio of $-1 < R < 1$, from the low ε measurements of P_l one can reconstruct A_y with 2% uncertainty.By projecting these limits to the $A_y(R)$ curves for the other ε (bottom of Fig. 13), one can reconstruct R independently for each of these ε points. Then, by projecting these results up at Fig. 13, the other two amplitudes can be reconstructed as functions of ε. The results of this procedure is shown at Fig. 14. Using this method there is no way to reconstruct the amplitudes at the lowest ε point. The uncertainties are big and one could recognize only a large ε dependence.

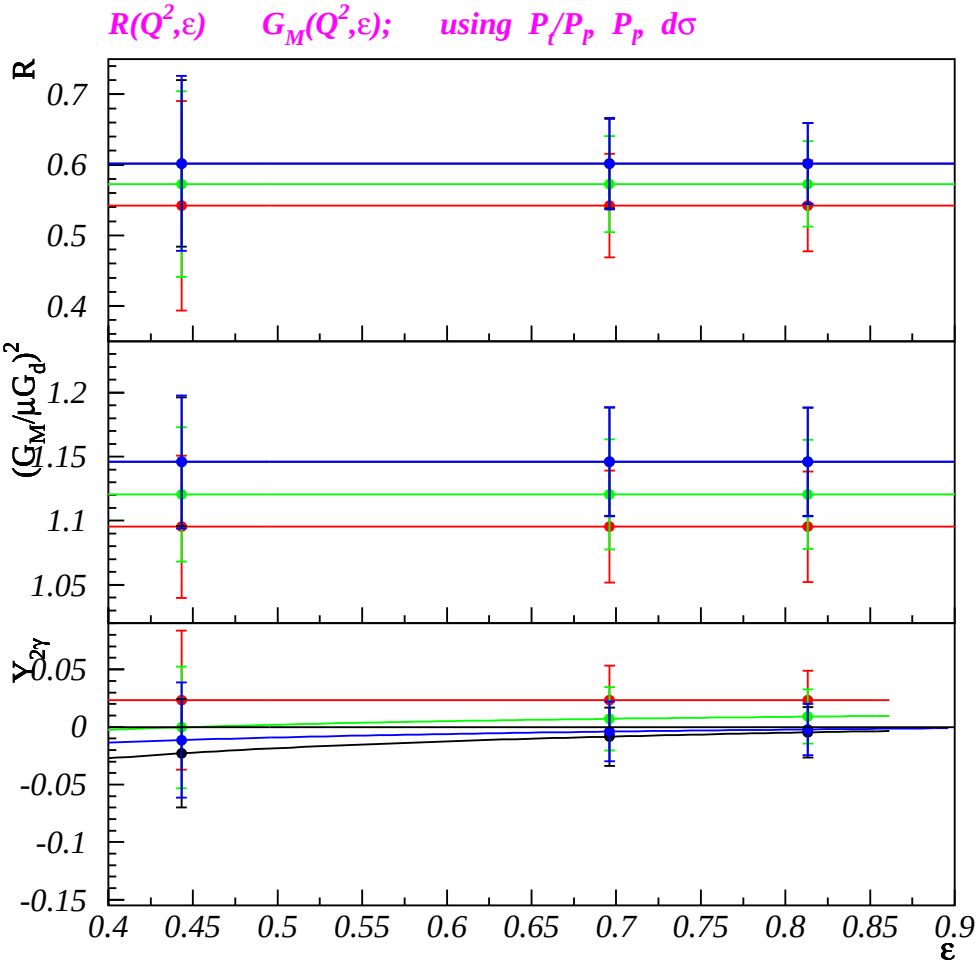

FIG. 14. Same as Fig. 11 but allowing both G_e/G_m and G_m to depend on ε.

III. A NOTE ON *ED* ELASTIC SCATTERING

In out letter of intent, LOI-03-101, we proposed to measure the induced polarization in both *ep* and *ed* elastic scattering. The measurements of *ed* elastic scattering are attractive, because TPEX might be larger than for the proton, due to the faster falloff of the deuteron form factor and the low excitation energy of the first inelastic state, and because the measurements potentially offer access to TPEX on the neutron. Simultaneously, we would measure the vector polarization transfer ratio P_x/P_z in *ed* elastic scattering. It yields a ratio of form factors, $(G_C + \frac{1}{3}\eta G_Q)/G_M$ and provides independent check on the extracted deuteron form factors using Rosenbluth separations. Additional measurements studying the dependence of p_y, P_x, and P_z on ε would be performed for the deuteron.

For this proposal, we have decided to focus solely on the proton measurement. We will return to the deuteron measurements at a more appropriate time in the future, after there is more understanding of TPEX on the proton and once the theoretical work on the deuteron, which is now being studied by a few theorists, is finished.

In a future proposal, in addition to the deuteron measurements, we will also include a few measurements on the proton at low Q^2, one of them will be at the same beam energy as the beam asymmetry measurement at Mainz A4 (854 MeV). The deuterons and low Q^2 protons have special requirements on the FPP analyzer thickness and material. Finally, we will repeat a kinematics of this proposal so we can measure the same induced polarization on both sides of the beam.

IV. ACKNOWLEDGMENT

We acknowledge very stimulating discussions with Franz Gross, and Andrei Afanasev.

---

[1] P. A. M. Guichon and M. Vanderhaeghen, Phys. Rev. Lett. **91**, 142303 (2003).

[2] L. Andivahis *et al.*, Phys. Rev. D **50**, 5491 (1994).

[3] J. Arrington, Phys. Rev. C **68**, 034325 (2003).

[4] M. K. Jones *et al.*, Phys. Rev. Lett. **84**, 1398 (2000); O. Gayou *et al.*,Phys. Rev. C **56**, 038202 (2001); O. Gayou *et al.*,Phys. Rev. Lett. **88**, 092301 (2002).

[5] Results from the Hall A "super-Rosenbluth" experiment 01-001 have been reported at several meetings, as have results from analysis of Hall C experiments.

[6] J. Gunion and L. Stodolsky, Phys. Rev. Lett. **30**, 345 (1973); V. Franco, Phys. Rev. D **8**, 826 (1973); R. Blankenbecker and J. Gunion, Phys. Rev. D **4**, 718 (1971).

[7] M. P. Rekalo, E. Tomasi-Gustafsson, and D. Prout, Phys. Rev. C **60**, 042202 (1999).

[8] S.P. Wells *et al.*, Phys. Rev. C **63**, 064001 (2001).

[9] Frank Maas, private communication.

[10] A. Afanasev, I. Akusevich, and N.P. Merenkov, hep-ph/0208260.

[11] L. Pentchev, C.F. Perdrisat, and V, Punjabi, to be published.

[12] P. G. Blunden, W. Melnitchouk, J. A. Tjon, Phys. Rev. Lett. **91**, 142304 (2003).

[13] A. Afanasev, I. Akushevich, A. Ilyichev, and N.P. Merenkov, Phys. Lett. B **514**, 269 (2001).

[14] J. Mar *et al.*, Phys. Rev. Lett. **21**, 482 (1968).

[15] H. C. Kirkman *et al.*, Phys. Lett. B **32**, 519 (1970).

[16] T. Powell *et al.*, Phys. Rev. Lett. **24**, 753 (1970).

[17] M. Vanderhaeghen, talk presented at Tucson Fall DNP Meeting, 2003.

[18] S.D. Drell and J.D. Sullivan, Phys. Lett. **19**, 516 (1965), first studied the effect on cross sections; A. Afanasev, talk presented at Workshop on Elastic Form Factors and Parity Violation, Athens, Greece, Oct. 6-7, 2003, and talk presented at Tucson Fall DNP Meeting, 2003 studied

the effect on cross sections and polarization observables.

[19] A. De Rujula, J.M. Kaplan and E. De Rafael, Nucl. Phys. B **53**, 545 (1973).

[20] A. Afanasev, private communication and M. Vanderhaeghen, private communication.

[21] P. Stoler, hep-ph/0307162.

[22] M. Christy, private communication; to be published (2003).

[23] J. Arrington, nucl-ex/0311019.